BJP British Journal of Pharmacology

DOI:10.1111/bph.13165
www.brjpharmacol.org

RESEARCH PAPER

Inhibition of breast cancer progression by a novel histone deacetylase inhibitor, LW479, by down-regulating EGFR expression

Jingjie Li[1]*, Tao Zhang[1,2]*, Feifei Yang[1], Yuan He[1], Fujun Dai[1], Dan Gao[1], Yihua Chen[1], Mingyao Liu[1,3] and Zhengfang Yi[1]

[1]*Shanghai Key Laboratory of Regulatory Biology, Institute of Biomedical Sciences and School of Life Sciences, East China Normal University, Shanghai, China,* [2]*Department of Orthopedics, Shanghai 1st People's Hospital, Shanghai Jiaotong University, Shanghai, China, and* [3]*Center for Cancer and Stem Cell Biology, Institute of Biosciences and Technology, Texas A&M University Health Science Center, Houston, TX, USA*

Correspondence
Dr Zhengfang Yi or Dr Yihua Chen or Dr Mingyao Liu, Institute of Biomedical Sciences, East China Normal University, 500 Dongchuan Road, Shanghai 200241, China. E-mail: zfyi@bio.ecnu.edu.cn; yhchen@bio.ecnu.edu.cn; mliu@ibt.tamhsc.edu

*These authors contributed equally to this work.

Received
16 October 2014
Revised
3 April 2015
Accepted
9 April 2015

BACKGROUND AND PURPOSE

Compounds targeting epigenetic events of tumours are likely to be an important addition to anticancer therapy. Histone deacetylase inhibitors (HDACI) have emerged as a promising novel class for therapeutic interventions associated with cancer, and many of them are currently in clinical investigation. Here, we assessed a novel hydroxamate-based HDACI, LW479, in breast cancer progression and explored its underlying mechanism(s).

EXPERIMENTAL APPROACH

LW479 was identified using the HDACI screening kit. Western blot and flow cytometry were used to analyse the biological effects of LW479 as a novel HDACI. The effects of LW479 were assessed in mouse models of spontaneous and experimental breast cancer. Co-immunoprecipitation, immunofluorescent staining and chromatin immunoprecipitation assays along with immunohistochemical analysis, were used to elucidate the molecular basis of the actions of LW479.

KEY RESULTS

LW479 was identified as a novel HDACI and showed marked cytotoxicity and induced apoptosis, as well as cell cycle arrest, in a panel of breast cancer cell lines. Intraperitoneal injections of LW479 markedly suppressed breast tumour growth and pulmonary metastasis in nude mice. LW479 also decreased levels of EGF receptors (EGFR) by blocking the binding of the transcription factor Sp1 and HDAC1 to the EGFR promoter region.

CONCLUSIONS AND IMPLICATIONS

Our data have elucidated the mechanisms underlying the inhibition by LW479 of tumour growth and metastasis, in models of breast cancer with aberrant EGFR expression. LW479 could be a candidate drug for breast cancer prevention.

Abbreviations

EGFR, EGF receptor; HATs, histone acetyltransferases; HDACI, histone deacetylase inhibitor; HDACs, histone deacetylases; IVIS, *In Vivo* Imaging System; SAHA, suberoylanilide hydroxamic acid

Tables of Links

TARGETS
Enzymes[a]
Akt
FAK, focal adhesion kinase
HDAC1, histone deacetylase 1
JNK
Catalytic receptors[b]
EGFR, EGF receptor

LIGANDS
Butyrate
Panobinostat
SAHA (suberoylanilide hydroxamic acid), vorinostat
Trichostatin A

These Tables list key protein targets and ligands in this article which are hyperlinked to corresponding entries in http://www.guidetopharmacology.org, the common portal for data from the IUPHAR/BPS Guide to PHARMACOLOGY (Pawson *et al.*, 2014) and are permanently archived in the Concise Guide to PHARMACOLOGY 2013/14 ([a,b]Alexander *et al.*, 2013a,b).

Introduction

Breast cancer is a serious health problem among women worldwide. It is estimated that 1.67 million women worldwide suffered from breast cancer in 2012, making breast cancer as the most common cancer type diagnosed in women. In addition, breast cancer is the most common cause of cancer death among women (http://globocan.iarc.fr/Default.aspx). Classically, breast cancer is considered to initiate from genetic defects that lead to the hyperactivation of oncogenes and hypoactivation of tumour suppressor genes. To date, accumulating evidence has indicated that epigenetic modifications also play important roles in breast cancer (Huang *et al.*, 2011).

Histone acetylation is the most widely studied among epigenetic modifications, apart from DNA methylation, in cancer development (Marks *et al.*, 2001; Esteller, 2007). The reciprocal activities of histone acetyltransferases (HATs) and histone deacetylases (HDACs) are critically involved in chromatin modification. HATs add acetyl groups to the N-terminal lysine residues of core histones, whereas HDACs remove acetyl groups from histones. Research on the association between HDACs and cancer development was started with the discovery that HDACs were the target of sodium butyrate, trichostatin A and trapoxin, which induced G1 and G2 phase cell cycle arrest and differentiation in certain mammalian cell lines (Ginsburg *et al.*, 1973; Altenburg *et al.*, 1976). Subsequent studies demonstrated that other compounds, initially identified as TGFβ mimetics or anti-tumour antibiotics, also exhibited potent inhibitory effect against HDACs (Su *et al.*, 2000; Glaser *et al.*, 2002). In recent years, many studies have suggested the involvement of HDACs in cancer initiation and progression. Several HDACs induced angiogenic stimulators and thus increased angiogenesis (Deroanne *et al.*, 2002; Rossig *et al.*, 2002; Sasakawa *et al.*, 2003). In addition, HDACs regulated the expression of metastasis-associated genes (Xu *et al.*, 2007). It is now widely accepted that HDACs are one of the more promising targets in cancer therapy.

Recently, low MW compunds targeting HDACs have received much attention as anticancer agents and some of them have demonstrated favourable anticancer activities in both preclinical and clinical settings (Bots and Johnstone, 2009; Khan and La Thangue, 2012). Aberrant activation of HDACs in breast cancer samples has been described (Byler *et al.*, 2014), and histone deacetylase inhibitors (HDACIs) as anticancer agents have shown therapeutic potential in breast cancer (Bots and Johnstone, 2009). HDACIs can overcome oestrogen receptor modulator/aromatase inhibitor resistance in oestrogen receptor (ER)-positive breast cancer (Munster *et al.*, 2011) and sensitize ER-negative breast cancer to hormone therapy (Jang *et al.*, 2004). Recently, Tate *et al.* (2012) demonstrated that the HDACI panobinostat (LBH589) selectively targeted triple-negative breast cancer (TNBC) cells *in vitro* and *in vivo*.

The human EGF receptor (EGFR/ErbB1) contains the first receptor tyrosine kinase to be identified and cloned and is a member of the ErbB family of receptor tyrosine knases. Upon ligand binding, the EGFR forms kinase-active homodimesr or heterodimers and induces its downstream signalling pathways (Avraham and Yarden, 2011). The EGFR plays pleiotropic roles in human cancer and overexpression of EGFR is observed in a wide range of solid tumours including breast cancer (Wheeler *et al.*, 2010). Aberrant EGFR in breast cancer correlates with aggressive clinical behaviour (Baselga, 2002) and increased EGFR was shown to be a predictor of ER-positive breast cancer risk (Pitteri *et al.*, 2010). Furthermore, EGFR dysregulation is more frequently detected in triple-negative breast cancer and inflammatory breast cancer, two subtypes of breast cancer with highly aggressive phenotypes (Masuda *et al.*, 2012). The 5′-regulatory region of the *EGFR* gene contains a GC-rich, TATA-less, CAAT-less, promoter and thus many transcription initiation sites are locates in the promoter region. A variety of DNA-binding factors including the transcription factor Sp1 have been identified as interacting with the *EGFR* promoter region. In addition, several Sp1 binding sites have been discovered and Sp1 is deemed necessary for basal transcription of the *EGFR* gene (Nishi *et al.*, 2002; Brandt *et al.*, 2006).

In our present study, we demonstrated that LW479, a novel HDACI, inhibited breast cancer progression in mouse models *in vitro* and *in vivo*. Further mechanistic studies

revealed that LW479 suppressed EGFR expression in breast cancer cells and that the low EGFR level may be ascribed to the disassociation of Sp1 and HDAC1 from the EGFR promoter. The ability of LW479 to block breast cancer growth and metastasis supports LW479 as a novel candidate for breast cancer therapy.

Methods

Synthesis, characterization and preparation of LW-479 and suberoylanilide hydroxamic acid (SAHA)

6-{2-[2-(3-Bromophenyl)-4-oxo-3-thiazolidinyl]phenoxy}-N-hydroxylhexanamide (LW479) and SAHA were synthesized in the Shanghai Key Laboratory of Regulatory Biology, East China Normal University. The synthetic route and purity analysis of LW479 are shown in Supporting Information Figs. S1–S3. SAHA was synthesized as described previously (Gediya *et al.*, 2005). Compounds were dissolved in DMSO and stored at –20°C as small aliquots.

Cell line and cell culture

Human breast cancer cell lines MDA-MB231 (hereafter designated as MDA-231), BT549, HCC1937 and MDA-MB468 (hereafter designated as MDA-468) were obtained from the ATCC and maintained in the complete growth media recommended. MDA-231 human breast cancer cells transfected with a reporter gene encoding luciferase (MDA-231-Luc) were a kind gift from Dr Qian Zhao at Shanghai Jiaotong University and grown in MEM (Gibco, Gaithersburg, MD, USA) with 1% non-essential amino acids and 10% FBS.

HDACI identification

HDACI activity assay was performed using the HDACI screening kit. Candidate HDACIs or SAHA were incubated with HeLa nuclear extracts or MDA-231 cell lysates and HDAC fluorometric substrate containing an acetylated lysine side chain at 37°C for 1 h. The lysine developer was then added to stop the reaction and the fluorescence was measured, using 350–380nm excitation and 440–460 nm emission. Three independent experiments were carried out in triplicate.

Western blotting

Western blotting was performed as described previously (Dong *et al.*, 2010). Cells were harvested with RIPA buffer containing 150 mM sodium chloride, 1% Triton X-100, 0.5% sodium deoxycholate, 0.1% SDS, 50 mM Tris and cocktails of protease and phosphatase inhibitors. Heat-denatured protein was then analysed by 8–15% SDS-PAGE and transferred onto PVDF membranes. Membranes were blocked with 5% BSA, incubated with specific primary antibodies and exposed to HRP-conjugated anti-rabbit or anti-mouse secondary antibody (Sigma, St. Louis, MO, USA). The chemiluminescence signals emanating from the membranes were detected by ECL reagent. Three independent experiments were carried out in triplicate.

MTS cell viability assay

MTS assay was performed according to the manufacturer's instruction (Promega, Madison, WI, USA). Breast cancer cells (5×10^3) were seeded in 96-well plates and, after incubation for 12 h; different concentrations of LW479 were added and incubated for another 48 h. Aqueous One Solution (20μL) was subsequently added and the absorption at 490 nm was measured by a microplate spectrophotometer. Three independent experiments were carried out in triplicate.

Cell cycle analysis

MDA-231 cells were plated in 6 cm dishes, treated with indicated concentrations of LW479 for 24 h and trypsinized. Cells were collected by centrifugation and then fixed in ice-cold 70% ethanol at 4°C for 24 h. After several PBS washes, fixed cells were resuspended in PBS containing RNase and PI solution and incubated at 37°C for 30 min in the dark. Cell cycle distribution was analysed by flow cytometry (BD Biosciences, Pasadena, CA, USA). Three independent experiments were carried out in triplicate.

Cell apoptosis detection

MDA-231 cells were cultured in 6 cm dishes in the presence of different concentrations of LW479 for 48 h. Cells were washed in PBS and resuspended in binding buffer (BD Biosciences) containing FITC-conjugated Annexin V and PI. Cell apoptosis was determined by a flow cytometer (BD Biosciences). Three independent experiments were carried out in triplicate.

Transwell invasion assay

Transwell invasion assay was performed using a modified Boyden chamber system (Millipore, Billerica, MA, USA) according to the manufacturer's instructions. After starvation overnight, MDA-231 cells were resuspended at 5×10^4 cells in 100 μL serum-free medium with or without indicated concentrations of LW479 and added to each transwell insert, pre-coated with 1 mg·mL^{-1} Matrigel. Serum-free medium (0.5 mL) or the same volume containing EGF (50 ng·mL^{-1}) was placed in each bottom well. Twelve hours post-seeding, non-invaded cells on the upper side of the transwell were removed using cotton swabs. Invaded cells on the undersurface were fixed with 4% paraformaldehyde and stained with 0.1% crystal violet. Images were acquired using an inverted microscope (Olympus, Tokyo, Japan) and cells were counted manually. Three independent experiments were carried out in triplicate.

Wound-healing migration assay

Wound-healing migration assay was performed by seeding cells in a 6-well plate as previously reported with modifications (Zhang *et al.*, 2012). When the cells were fully confluent, cells were starved overnight and a 'wound' was made by a 100 μL pipette tip. Fresh serum-free medium or that containing EGF (50 ng·mL^{-1}) and different concentrations of LW479 were added. Cells were allowed to migrate for 12 h and fixed with 4% paraformaldehyde. Images were taken by an inverted microscope (Olympus) and migrated cells were counted manually. Three independent experiments were carried out in triplicate.

Immunofluorescence (IF) assay

MDA-231 cells were seeded on gelatin-coated coverslips and treated with different concentrations of LW-479 for 24 h before stimulation with EGF (50 ng·mL^{-1}) for 30 min. Cells

were fixed with 4% paraformaldehyde for 15 min, permeabilized with 0.1% Triton X-100 for 10 min and blocked with 0.5% BSA for 30 min. Target proteins in cells were visualized by incubation with the corresponding antibodies overnight at 4°C, followed by incubation with FITC-conjugated secondary antibodies for 1 h. Rhodamine-conjugated phalloidin and 4′, 6-diamidino-2-phenylindole were subsequently used to localize F-actin and nucleus. Images were acquired with a confocal microscope (Leica, Wetzlar, Germany). Three independent experiments were carried out in triplicate.

RT-PCR

RNA samples from cells were prepared using Trizol (Invitrogen, Carlsbad, CA, USA) according to the manufacturer's protocols. Total RNA (1μg) was converted to cDNA using oligo dT primer. The relative expression of EGFR was analysed by RT-PCR with GAPDH as an internal control. The primer sequences used for PCR for EGFR were 5′-CCTGGT CTGGAAGTACGCAG-3′ and 5′-CTTCGCATGAAGAGGCC GAT-3′. PCR products were separated on 1.2% agarose gel and then stained with ethidium bromide. Three independent experiments were carried out in triplicate.

Haematoxylin and eosin (H&E) staining and immunohistochemical (IHC) analysis

Primary tumours, lungs or other organs were freshly excised from mice and fixed in 4% paraformaldehyde overnight prior to paraffin embedding. Sections (4 μm) were then deparaffinized for H&E and IHC staining. For IHC, deparaffinized slides were subjected to epitope retrieval in sodium citrate solution and blocked in 3% H_2O_2, then probed with specific antibodies (EGFR and acetyl-H3) at 4°C overnight. Immunodetection was visualized by a diaminobenzidine detection kit.

Three-dimensional top culture assay

Three-dimensional top culture assay was conducted as previously reported (Lee *et al.*, 2007). Growth factor-reduced Matrigel was thawed at 4°C overnight. Matrigel solution (80 μL per well) was added to 48-well plates and left at 37°C for 30 min to solidify. A total of 1.5×10^4 MDA-231 cells were resuspended in 100 μL serum-free medium followed by seeding on solidified Matrigel. Fifteen minutes post cell attachment, 100 μL serum-free media containing 10% Matrigel indicated concentrations of LW-479 and EGF was added on top of the plated culture. The on-top Matrigel medium was replaced every 2 days. All experiments were performed in triplicate and repeated at least three times.

Co-immunoprecipitation

Co-immunoprecipitation was performed as previously reported (Dai *et al.*, 2012). MDA-231 cells were treated with or without LW479 for 24 h and nuclear lysates were prepared. Equal amount of nuclear extracts was incubated with anti-Sp1 and anti-HDAC1 antibodies for 12 h at 4°C. The immunoprecipitated pellets were then incubated with protein A/G agarose beads followed by five washes with wash buffer.

Chromatin immunoprecipitation (ChIP) assay

ChIP assay was performed as previously described (Dong *et al.*, 2010). MDA-231 cells were cross-linked in 1% formaldehyde in PBS for 10 min, followed by adding glycine to quench unreacted formaldehyde. Cell lysates were then collected with cold lysis buffer for ChIP and sonicated to obtain chromatin with an average fragment size of 500 bp. The chromatin samples were precleared with protein A/G agarose/salmon sperm DNA beads for 1 h and then immunoprecipitated with antibodies against IgG, HDAC1 and Sp1. After 12 h of incubation, the samples were incubated with protein A/G agarose beads for 2 h. After five sequential washes, cross-links were eluted with elution buffer plus proteinase K and reversed at 65°C for 12 h. DNA was extracted with phenol-chloroform. Immunoprecipitated DNA was analysed by real-time PCR.

siRNA-mediated knockdown

MDA-231 cells were seeded in a 6-well plate 24 h before transfection. siRNAs targeting *HDAC1* or non-specific control (siControl) were transfected using lipofectamine 2000 reagent (Life Technologies, Carlsbad, CA, USA). The sequences of siRNAs against *HDAC1* were 5′-TAAGGTT CTCAAACAGTCG-3′ and 5′-AAGCCGGUCAUGUCCAA AGUA-3′ (Mottet *et al.*, 2007; Pulukuri *et al.*, 2007).

Luciferase reporter gene assay

The EGFR promoter–luciferase construct was transiently transfected into MDA-231 cells. Briefly, MDA-231 cells were seeded in 24-well plates and cultured for 24 h. Cells were co-transfected with the EGFR promoter–luciferase construct and *Renilla* luciferase, according to the manufacturer's instructions (Promega). The cells were then exposed to LW479 for 24 h. Luciferase activity was measured and normalized against *Renilla* luciferase activity.

EMSA

EMSA was performed using Odyssey Infrared Sp1 EMSA Kit (LI-COR Biosciences, Lincoln, NE, USA) following the manufacturer's protocol. In brief, nuclear extracts from MDA-231 cells were prepared and incubated with Sp1 IRDye™ 700 infrared dye-labelled oligonucleotides (LI-COR Biosciences). The protein–DNA complex was applied to 6.6% native polyacrylamide gels. The gels were visualized with Odyssey infrared system.

Animals

All animal care and experimental studies were conducted according to the guidelines and approval of the Animal Investigation Committee of the Institute of Biomedical Sciences and School of Life Sciences, East China Normal University. Studies with animals are described in compliance with the ARRIVE guidelines for reporting experiments involving animals (Kilkenny *et al.*, 2010; McGrath *et al.*, 2010).

BALB/c athymic nude mice and BALB/c mice were bred and housed at the animal centre in East China Normal University [21°C, 55% humidity, on a 12 h light/dark cycle (SPF)]. The total numbers used in each experiment were female BALB/c athymic nude mice in the spontaneous metastasis model, 32; female BALB/c athymic nude mice in the experimental metastasis model, 28; female BALB/c mice in toxicity study, 15.

Xenograft animal studies

Xenograft animal studies were performed as described previously (Zhang *et al.*, 2014).

Spontaneous metastasis mouse model

Female nude mice, 6–8 weeks of age, received orthotropic inoculations in the no. 4 inguinal mammary fat pad with 50 μL of MDA-231-Luc cell suspension containing 1×10^6 cells. Treatment began 1 week after tumour cell injection when palpable tumours had formed. Mice were allocated into four groups for treatment based on the *in vivo* imaging results on treatment day 0 using the Xenogen *In Vivo* Imaging System (IVIS; Xenogen Corporation, Danville, CA, USA). Tumour growth was measured weekly by monitoring tumour length (L) and width (W). Tumour volume was calculated from $L \times W^2 \times 0.52$. Each group contained eight mice. When the study was terminated, various organs were collected and imaged by IVIS to detect distant metastasis.

Experimental metastasis mouse model

A total of 1×10^6 MDA-231-Luc cells in 100 μL PBS were injected into the nude mice at the age of 6–8 weeks through the tail vein. Mice given tumour cells on day 0 were assigned into four groups for treatment with or without i.p. injections of indicated doses of LW-479 or SAHA (n = 7 per group). Real-time whole body images were acquired using the Xenogen IVIS. Lung metastasis was expressed in units of photons s^{-1} cm^{-2} sr^{-1}.

Toxicity study of LW479

For potential toxicity testing, female BALB/c mice (6–8 weeks of age) were randomly assigned to three groups (n = 5 per group) and received i.p. injections of DMSO or LW479 (40 mg·kg^{-1}) or SAHA (40 mg·kg^{-1}) once a day. Body weight was monitored every 6 days. On day 30, mice were killed and major organs were freshly dissected. Histological examinations were carried out using H&E staining.

Data analysis

Results are expressed as mean ± SE. Groupwise comparisons were determined by Student's t-test. All experiments were performed at least three times, except for the whole animal experiments. P-values less than 0.05 were considered statistically significant.

Materials

Growth factor-reduced Matrigel was purchased from BD Biosciences. HDACi screening kit was obtained from BioVision (Milpitas, CA, USA).

Antibodies for Western blot, immunofluorescence and IHC included phospho-EGFR/EGFR, phospho-FAK/FAK, phospho-JNK/JNK, phospho-AKT/AKT, acetyl-histone H3, histone H3, acetyl-histone H4, HDAC1, HDAC2, HDAC3, HDAC4 and HDAC6 (Cell Signaling Technology, Danvers, MA, USA); Sp1 and acetyl-lysine (Millipore); Paxillin (BD Transduction Laboratories, Pasadena, CA, USA); and β-actin (Sigma).

Results

LW-479 is identified as a HDACI

LW479 was discovered using the HDACI drug-screening kit in our internal chemical library. The chemical structure of LW479 is shown in Figure 1A, with the details of the synthetic route and identification provided in Supporting Information Figs. S1–S3. As shown in Figure 1B, LW479 was a potent inhibitor of HDAC enzyme activity, in HeLa cell nuclear extracts and MDA-231 cell lysates. Treatment with 10 μM of LW479 resulted in marked increases in histone H3 and H4 acetylation, the characteristic indicators of HDAC inhibition, in a panel of breast cancer cell lines (Figure 1C and D and Supporting Information Fig. S4A). In parallel, we used total histone H3 as a loading control. The HDAC inhibition could also be observed by the varying degrees of reduction of individual HDACs (HDAC1-HDAC4, HDAC6) (Figure 1C). HDACIs are known for their ability to selectively block proliferation, induce apoptosis and cell cycle arrest in cancer cells (Minucci and Pelicci, 2006). The effect of LW479 was thus tested on these aspects. MTS assay (Figure 1E) showed LW479-inhibited proliferation of all four types of breast cancer cells in a dose-dependent manner. The anti-proliferation characteristic of LW479 was similar to that of SAHA (Supporting Information Fig. S5). Annexin V/PI staining in Figure 1F indicated enhancement of apoptosis by LW479. In addition, we performed annexin V/PI assays and caspase activity assays and found that LW479 (10 μM) induced cell apoptosis and, using Western blots, up-regulated the expression of cleaved caspase 3 and down-regulated the expression of caspase 3 (Supporting Information Fig. S4B and C). Furthermore, flow cytometry analysis showed that LW479 induced G2/M phase arrest in MDA-231 cells (Figure 1G). Results from all of these assays suggest that LW479 acts as a HDACI.

LW479 silences EGFR expression in breast cancer cells through disrupting Sp1 and HDAC1 binding to EGFR promoter

Aberrant EGFR expression has been commonly observed in breast cancers (Pitteri *et al.*, 2010) and the EGFR profiles have prognostic value (Baselga, 2002). As shown in Figure 2A, treatment of four breast cancer cell lines with LW479 (1–20 μM) decreased the levels of EGFR protein, in a dose-dependent fashion. Because the EGFR protein expression was so markedly reduced by LW479, we queried whether LW479 treatment was attenuating EGFR at the mRNA level. MDA-231 cells were treated with increasing concentrations of LW479 and conventional RT-PCR revealed the suppression of EGFR mRNA (Figure 2B). These data suggested that the diminished EGFR protein expression may be, in part, caused by a decrease in mRNA levels. A earlier study demonstrated abnormal expression of individual HDACs in tumour samples and overexpression of HDAC1 is seen in breast carcinoma (Bolden *et al.*, 2006). To examine the role of HDAC1 in EGFR expression, endogenous HDAC1 was knocked down in MDA-231 cells by treatment with specific siRNAs directed against *HDAC1* (Figure 2C). In HDAC1 knockdown cells, a diminished level of EGFR expression was observed when compared with cells transfected with control siRNA (Figure 2C). Basal EGFR gene transcription is modulated by the transcription factor Sp1 (Brandt *et al.*, 2006) and post-translational modifications such as acetylation are known to influence the transcriptional activity of Sp1 (Tan and Khachigian, 2009). Aberrant recruitment of HDAC1 to promoters through interacting with Sp1 has shown to regulate gene transcription (Varshochi *et al.*, 2005). To determine whether Sp1 was

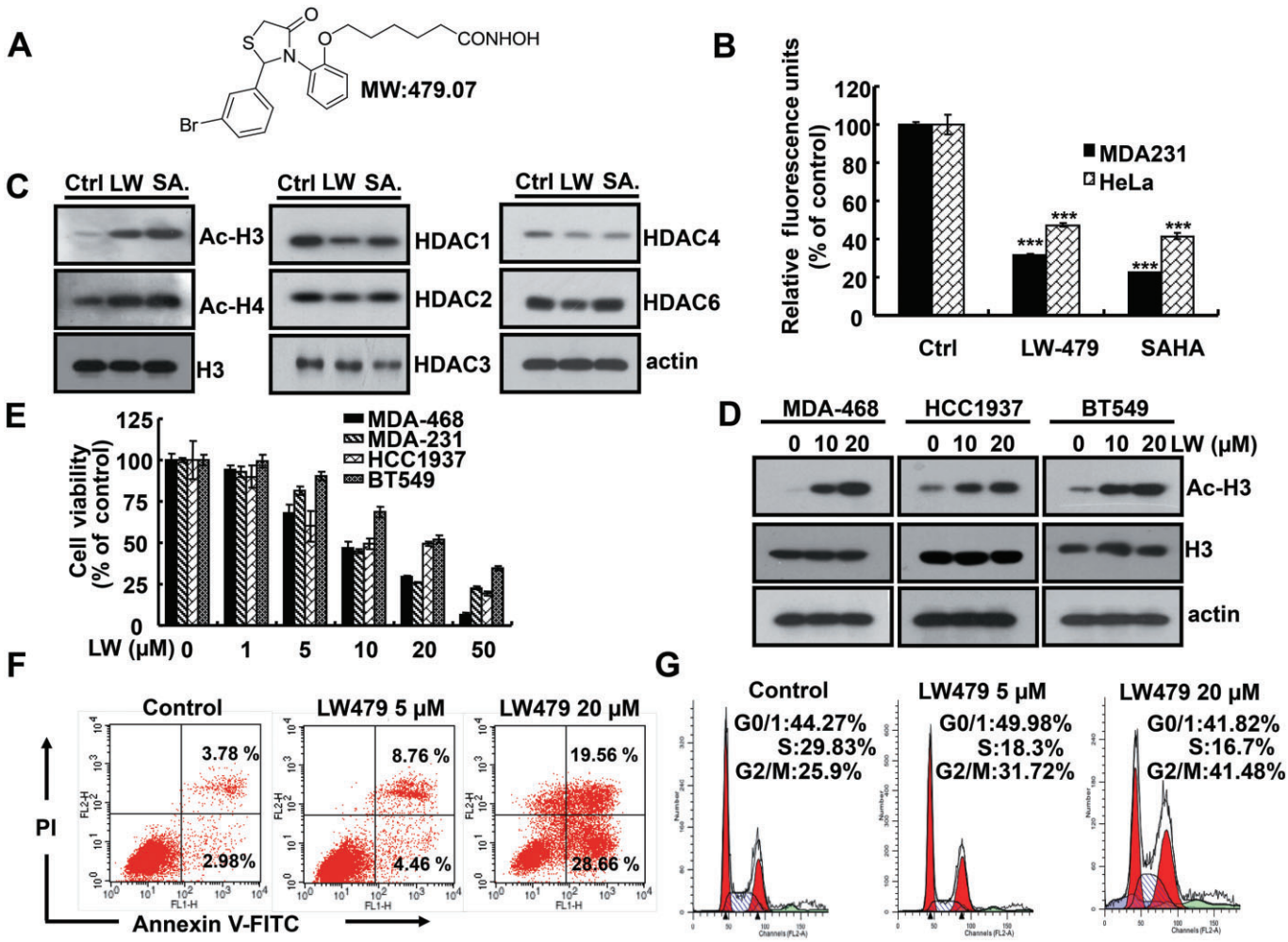

Figure 1

LW479 is identified as a HDACI. (A) Chemical structure of LW479. (B) HeLa cell nuclear extracts and MDA-231 cell lysates were treated with 10 μM LW479 or SAHA followed by co-incubation with HDAC fluorometric substrate at 37°C for 1 h. The lysine developer was added to stop the reaction, and the fluorescence units was measured at Ex/Em 350–380/440–460 nm. SAHA was used as a positive control. (C) MDA-231 cells were exposed to 10 μM LW479 (LW) or SAHA (SA) for 24 h and then whole cell lysates were probed using indicated antibodies by Western blot; total histone 3 as loading control. (D) Acetylated histone 3 (Ac-H3) protein level was induced by LW479 in various breast cancer cell lines. (E) Different breast cancer cell lines were treated with increasing concentrations of LW479 for 48 h and MTS assay was conducted. (F) MDA-231 cells were left untreated or treated with LW479 at the indicated doses for 48 h. Apoptotic cells were labelled with annexin V and PI and analysed by flow cytometry. (G) MDA-231 cells were treated with different concentrations of LW479 and incubated for 24 h. Cell population distribution was determined following PI staining and further analysed by flow cytometry. ***$P < 0.001$ versus control.

acetylated or bound to HDAC1 and what effect LW479 had on these interactions, cell nuclear lysates were prepared and then immunoprecipitated with anti-Sp1 or anti-HDAC1 antibodies followed by Western blot analysis with antibodies against acetyl-lysine or Sp1. As shown in Figure 2D, one band located at ~90 kD could be recognized by anti-acetyl-lysine antibody in anti-Sp1 immunoprecipitants in the LW479 (20 μM) treated group. After normalization for the amount of protein present, we found a decreased binding of HDAC1 to Sp1, in the presence of LW479. The IF assay also showed a reduced co-localization between HDAC1 and Sp1 in nuclei of cells treated with LW479 (Figure 2E). To assess if the effect of LW479 on the interaction between HDAC1 and Sp1 modulated their binding to the EGFR promoter, we performed quantitative ChIP assays. There are four Sp1 recognition sites in the EGFR promoter region (–329/–320, –310/–301, –221/–212 and –99/–90) (Liu *et al.*, 2005). We designed primers to cover the regions –329/–320 and –310/–301 in the EGFR promoter. A high level of HDAC1 was observed at EGFR promoters in untreated cells, whereas LW479 induced the dissociation of HDAC1 from the EGFR promoter (Figure 2F). Similar results was obtained when the recruitment of Sp1was tested (Figure 2F). Moreover, knockdown of Sp1 caused a decreased level of EGFR mRNA and protein in MDA-231 cells (Supporting Information Fig. S6A and B). Overexpression of Sp1 in cells treated with LW479 attenuated the reduction of EGFR mRNA and protein expression (Supporting Information Fig. S6C and D). In addition, in order to determine that the

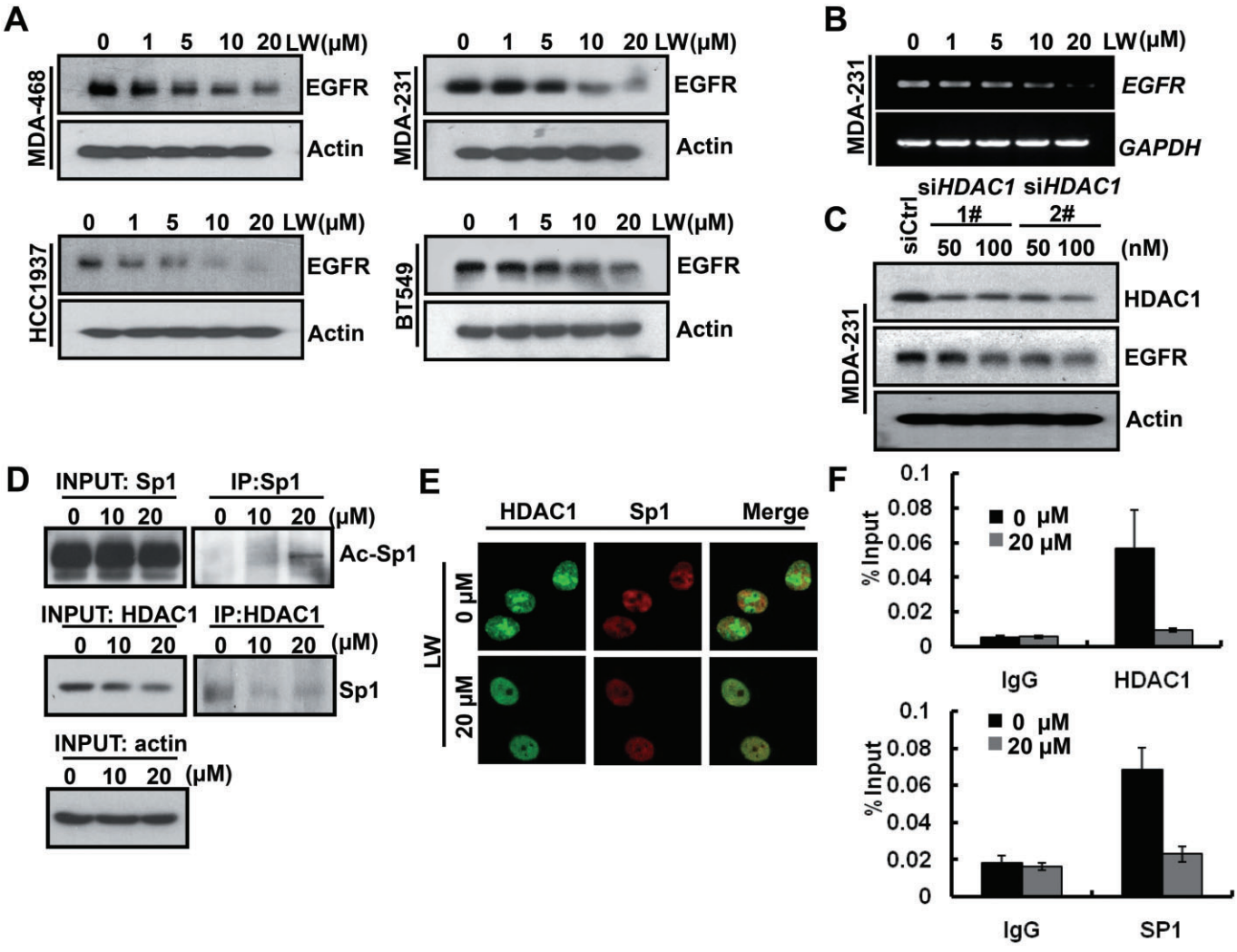

Figure 2

LW479 silences EGFR expression in breast cancer cells through disrupting HDAC1 and Sp1 binding to the EGFR promoter. (A) A panel of breast cancer cell lines were incubated with or without LW479 for 24 h; whole cell lysates were analysed by immunoblotting for EGFR and β-actin. (B) MDA-231 cells were treated with LW479 for 24 h and then analysed for EGFR mRNA expression by RT-PCR. (C) MDA-231 cells were transfected with siRNAs targeting HDAC1 (siHDAC1 1# and 2#) or non-specific control (siCtrl). Western blot analysis was used to detect the specific knockdown of HDAC1. HDAC1 knockdown repressed EGFR expression. (D) MDA-231 cells were pre-incubated with LW479 and nuclear extracts were prepared. The immunoprecipitation was performed using anti-Sp1 and anti-HDAC1 antibodies. The immunoprecipitated pellets were analysed by immunoblotting with anti-acetyl-lysine and anti-Sp1 antibodies. (E) MDA-231 cells treated with or without LW479 were stained for HDAC1 (green) and Sp1 (red). (F) MDA-231 cells were incubated with LW479 and the proteins were cross-linked with DNA and analysed by ChIP assay with anti-HDAC1 and anti-Sp1 antibodies.

reduced level of EGFR was due to transcriptional inhibition, cells were transiently transfected with the EGFR promoter–luciferase construct and treated with or without LW479 for 24 h. EGFR promoter activity was drastically reduced by LW479 (Supporting Information Fig. S6E), suggesting that the transcriptional inhibition leads to the decreased EGFR expression. Using EMSA assay, we demonstrated that LW479 or knockdown of Sp1 suppressed the endogenous Sp1 binding activity (Supporting Information Fig. S6F). These data indicated that the diminished interaction between HDAC1 and Sp1 induced by LW479 contributes importantly to the LW479-induced suppression of EGFR.

LW479 blocks EGF/EGFR signalling pathway and EGF-stimulated motility

We next examined whether the downstream targets of the EGF/EGFR signalling cascade were also inhibited by LW479. Although the phosphorylation of EGFR, FAK, Akt and JNK was clearly increased by stimulation of the cells by upon EGF stimulation, LW479 repressed their activation in a dose-dependent manner (Figure 3A), and this blockade of the EGF/EGFR signalling pathway by LW479 could be an indirect consequence of inhibiting EGFR transcription. Previous studies have demonstrated that dysregulated EGFR and

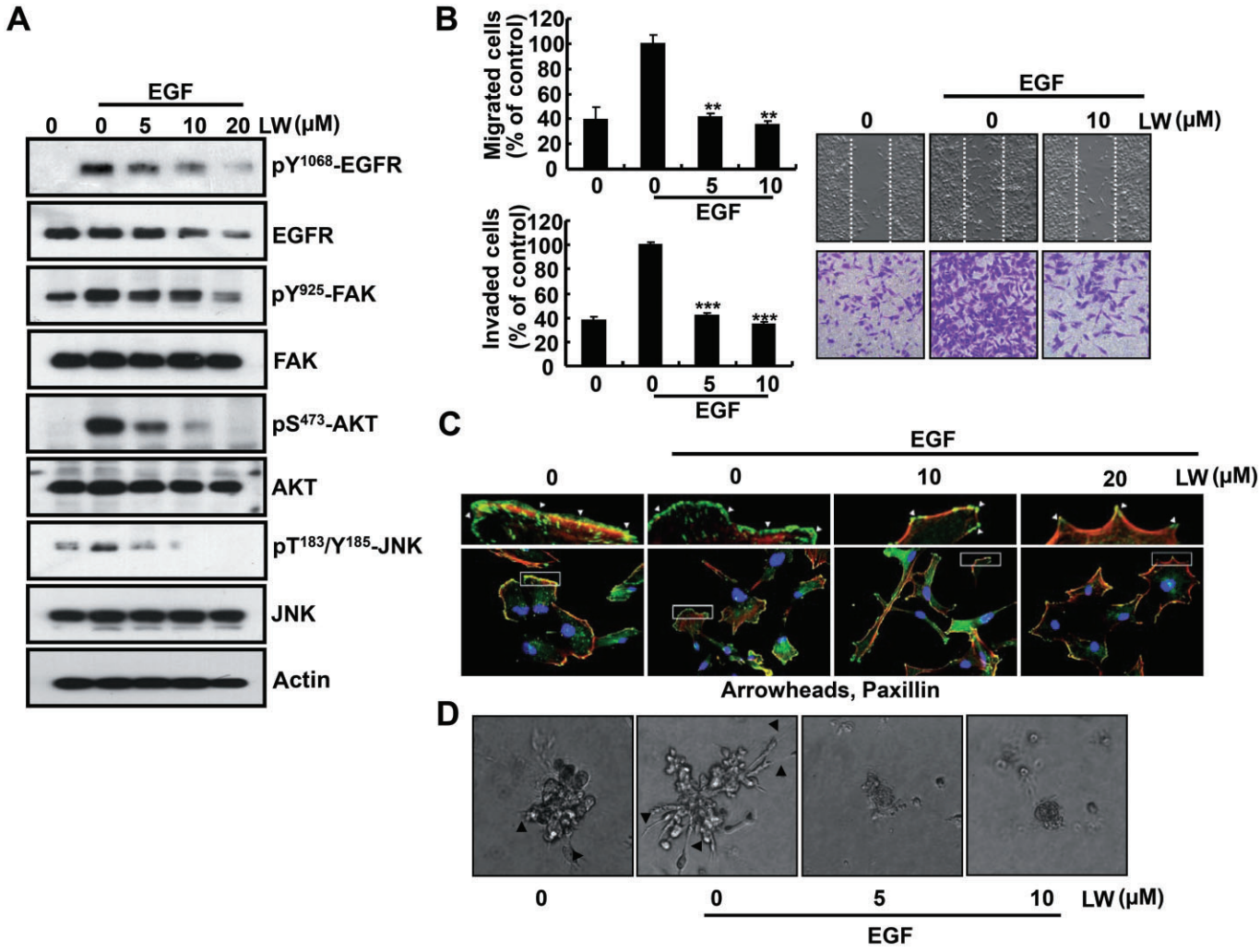

Figure 3

LW479 blocks EGF/EGFR signalling pathway and EGF-stimulated motility. (A) MDA-231 cells were pretreated with the indicated concentrations of LW479 for 24 h and then stimulated with EGF (50 ng·μL^{-1}) for 30 min. Whole cell extracts were prepared and analysed by Western blotting, using the relevant antibodies. (B) Confluent MDA-231 cells in 6-well plates were scratched to create a wound and starved in serum-free medium overnight followed by exposure to EGF and different concentrations of LW479. Images were taken after 12 h of incubation at 37°C (upper right). Cell migration was quantified manually (upper left). MDA-231 cells (1×10^5) were resuspended in serum-free medium and seeded into the upper side of the transwell inserts precoated with Matrigel. Increasing concentrations of LW479 and EGF (50 ng·μL^{-1}) were added in the bottom well. Images were obtained after 12 h of incubation (lower right). Inhibition of cell invasion by LW479 was expressed as % untreated control. (C) MDA-231 cells were treated with LW479 followed by 30 min of stimulation with EGF. Cells were fixed, permeabilized and incubated with anti-Paxillin antibody (green) and phalloidin (red). Cell nuclei were stained with DAPI. (D) MDA-231 cells were seeded onto solidified Matrigel. Serum-free medium (0.1mL) containing 10% Matrigel plus different concentrations of LW479 and EGF was added. After 4 days, culture cells were photographed using an inverted microscope. Arrow heads indicated invasive structures. $^{**}P < 0.01$; $^{***}P < 0.001$ versus control.

EGF-induced signalling promote tumour cell motility, invasion and metastasis (Lu *et al.*, 2001). As we had found that LW479 down-regulated EGFR at protein and mRNA level (Figure 2A and B), we tested the effects of LW479 on EGF-directed migration and invasion. As shown in Figure 3B, LW479-treated cancer cells were unable to respond to EGF stimulus to migrate and invade (Figure 3B). The activation of cancer cell focal adhesions by soluble growth factors plays pivotal roles in cell motility (Turner, 2000). Our data showed that LW479 impaired EGF-induced formation of focal adhesion, as can be seen from the reduced focal adhesion adaptor protein paxillin (Figure 3C).

Three-dimensional culture systems provide structural and functional aspects of cancer progression. Unlike monolayer cultures, mammary epithelial cells grown in three-dimensional systems reproduce the mammary glandular structure and many other features of breast epithelium *in vivo* (Lee *et al.*, 2007). Moreover, malignant breast epithelial cells

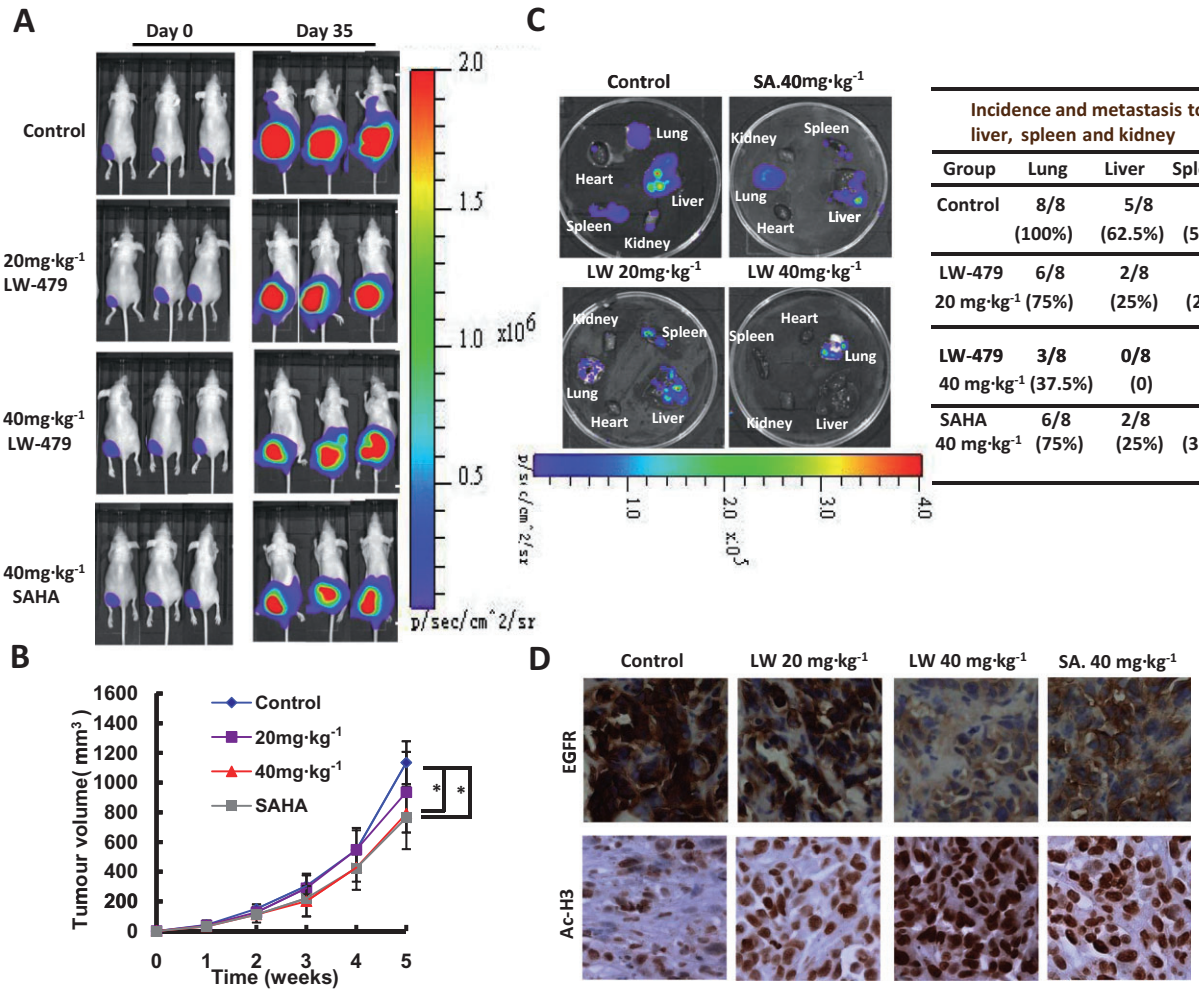

Incidence and metastasis to the lung, liver, spleen and kidney

Group	Lung	Liver	Spleen	Kidney
Control	8/8 (100%)	5/8 (62.5%)	4/8 (50%)	2/8 (25%)
LW-479 20 mg·kg^{-1}	6/8 (75%)	2/8 (25%)	2/8 (25%)	1/8 (12.5%)
LW-479 40 mg·kg^{-1}	3/8 (37.5%)	0/8 (0)	0/8 (0)	0/8 (0)
SAHA 40 mg·kg^{-1}	6/8 (75%)	2/8 (25%)	3/8 (37.5%)	0/8 (0)

Figure 4

LW479 prevents breast tumour growth and spontaneous metastasis. (A) MDA-231-Luc cells were injected into the mammary fat pad of female nude mice, resulting in a primary breast tumour. Real-time images on treatment day 0 and day 35 were acquired using the Xenogen IVIS. (B) Primary tumour was monitored weekly by a digital calliper. (C) *Ex vivo* bioluminescence images were obtained in each group to determine the effects of LW479 against distant metastasis. Metastasis incidence in distant organ was quantified. (D) Primary tumours were removed at the end of the experiment, fixed and paraffin embedded. Four micrometre Sections (4μm) were analysed by IHC using anti-EGFR and anti-acetyl-H3 antibodies. *P < 0.05 versus control.

invade the surrounding matrix in three-dimensional cultures and the invasive stellate structure can be easily observed by microscopy (Lu *et al.*, 2009). In our three-dimensional cultures, using growth factor-reduced Matrigel, LW479 inhibit EGF-induced breast cancer cell invasion, as few cells escaped from the acini and invaded the surrounding Matrigel (Figure 3D). These data demonstrated that LW479 impaired EGF-induced formation of focal adhesion and invasive structures, in three-dimensional cultures.

LW479 is effective in preventing breast tumour growth and spontaneous metastasis

To test the suppressive effects of LW-479 on breast cancer progression, we used a model in which MDA-231 cells encoding a luciferase reporter gene were injected into the mammary fat pad of nude mice. Bioluminescent images from this model on day 0 and day 35 are shown in Figure 4A. Mice treated with LW479 (40 mg·kg^{-1}) showed a marked reduction in tumour volume (Figure 4B). On day 35, the major organs of all groups of mice were removed and imaged for tumour presence. As shown in Figure 4C, only three mice in LW479 (40 mg·kg^{-1}) group were found to bear lung metastasis and no other distant metastasis were observed. In contrast, the untreated group progressed in a more aggressive manner: all mice developed lung metastases, five of the eight mice had liver metastases, four had spleen metastases and two had kidney metastases. Histological examination of these mice showed that the decreased tumour growth was accompanied by reduced expression of EGFR (Figure 4D, upper row). We also measured histone acetylation, within the tumour. In accord with the *in vitro* data, treatment with LW479 (40 mg·kg^{-1}) for 35 days significantly increased acetylation of histone H3 (Figure 4D, lower row).

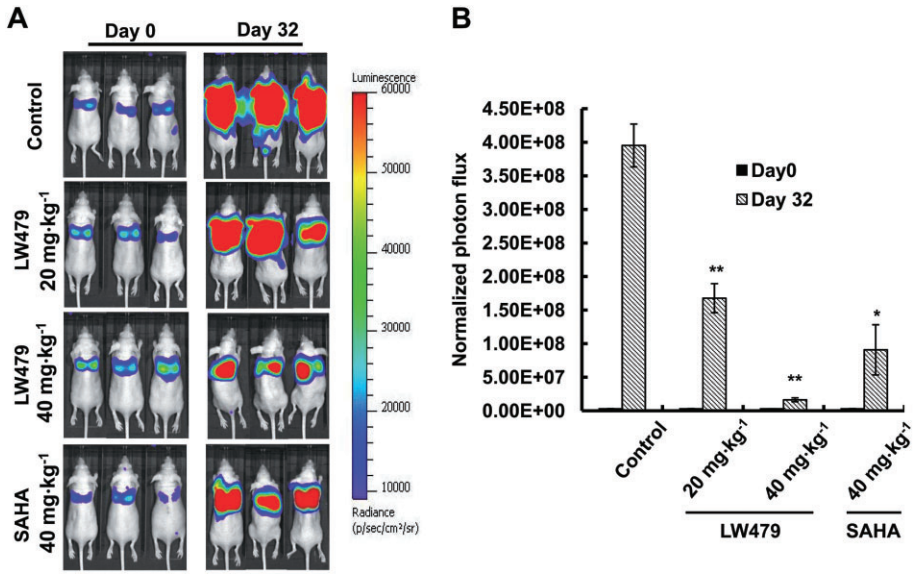

Figure 5

LW479 attenuates breast cancer metastasis to the lung. (A) MDA-231-Luc cells were inoculated i.v. into nude mice. Mice were assigned to four groups and received treatment. Lung colonization was assessed by Xenogen IVIS on day 0 and day 32. (B) Normalized bioluminescence quantification on day 0 and day 32. *$P < 0.05$ versus control; **$P < 0.01$.

LW479 attenuates breast cancer metastasis to the lung

To assess the anti-metastatic effects of LW479, we used a model with MDA-231-Luc cells injected i.v. in female nude mice. As shown in Figure 5A and B, treatment with LW479 (40 mg·kg^{-1}) markedly decreased lung metastases, achieving about 90% inhibition relative to the untreated control group, on day 32.

Toxicity test of LW479

To investigate the systemic toxicity of LW479, female BALB/c mice were given DMSO (vehicle), LW479 (40 mg·kg^{-1}) or SAHA (40 mg·kg^{-1}) for 30 days. Body weight was measured every 6 days over the treatment period. No loss of weight was observed in LW479-treated group compared with untreated or DMSO-treated group (Supporting Information Fig. S7). To further assess the toxicity of LW479, all mice were killed on day 30 and the major organs were fixed and paraffin embedded for H&E staining. Histological analysis revealed that LW479 showed no obvious damage to major organs including brain, heart, lung, liver, spleen and kidney (Figure 6). Our results indicated that LW479 caused no systemic toxicity to mice at the test concentrations.

Discussion

Numerous studies have revealed HDACs as excellent targets for cancer therapy and more than 20 different HDACIs are currently in clinical trials (http://clinicaltrials.gov/). In this report, we have identified a novel HDACI, LW479, and investigated the molecular mechanisms underlying the anti-breast cancer effects of this compound .

We demonstrated that LW479 inhibited HDAC activity using a HDACI screening kit. We further found that LW479 induced substantial increases in HDAC-related biomarkers, such as histone H3 and H4 acetylation, and abolished the expression of individual HDACs. HDACIs have been reported to induce apoptosis and cell cycle arrest in cancer cells. We demonstrated that LW479 sensitized breast cancer cells to apoptosis and caused G2/M phase cell cycle arrest. These results suggested that LW479 acts as a novel pan-HDACI.

EGFR is a member of the ErbB family that is frequently dysregulated in a variety of human epithelial cancers, including NSCLC, colorectal cancer, pancreatic cancer, brain cancer and breast cancer (Wheeler *et al.*, 2010). Many reports have described the importance of the EGFR in breast cancer (Baselga, 2002; Pitteri *et al.*, 2010; Masuda *et al.*, 2012). In our studies, we found that LW479 decreased the protein and mRNA levels of EGFR in breast cancer cells and the altered expression of EGFR protein may be a consequence of the reduced mRNA level. The regulation of EGFR by HDACIs has been reported in other studies. For instance, SAHA attenuated EGFR expression in ER-negative breast cancer cells (Zhou *et al.*, 2009) and diminished expression of EGFR was also found in colorectal cancer cells after SAHA treatment (Chou *et al.*, 2011). However, exactly how HDACIs affect the EGFR level in distinct cell types has ont been defined. The transcription factor Sp1 that regulates basal transcription of the EGFR gene is ubiquitously expressed and the effects of HDAC inhibition on Sp1 may be involved.

Although EGFR was known to be down-regulated by HDACIs in breast cancer cells, the mechanism involved in this down-regulation was not investigated. As noted earlier, the universally expressed transcription factor Sp1 is a key regulator for EGFR transcription. Sp1 recruits HDAC1 to the

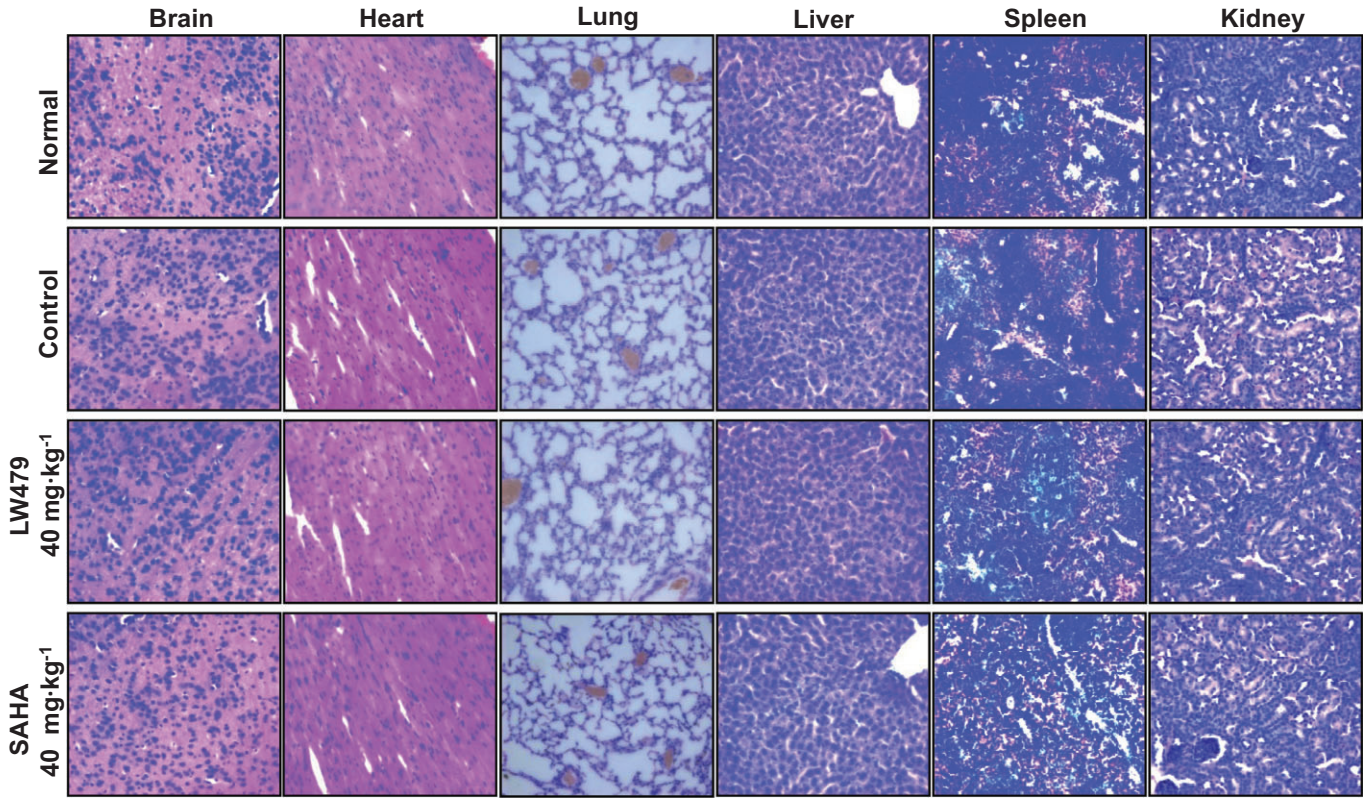

Figure 6
LW479 shows no systemic toxicity in mice. Major organs from the different groups of animals were stained with H&E.

promoter of regulated genes and mounting evidence indicates that the post-translational modifications (phosphorylation, acetylation, sumoylation, etc.) can influence the transcription activity of Sp1. Like many other non-histone cellular proteins, Sp1 is the target of acetylation events by HDACs (Schrump, 2009). Our results revealed that Sp1 was, constitutively, at low levels of acetylation in MDA-231 cells and this acetylation was increased by LW479 treatment. In addition, the interaction between Sp1 and HDAC1 was disrupted. LW479 also reduced the binding of Sp1 as well as that of HDAC1 to the EGFR promoter, leading to the transcriptional suppression of EGFR (Supporting Information Fig. S9). These data together indicated that suppression of EGFR by LW479 may involve the inhibition of HDAC1, which in turn up-regulates the acetylation level of Sp1. Acetylation has shown to be involved in protein–protein interaction (Arnesen, 2011). Acetylated Sp1 may be unfavourable for its interaction with HDAC1 in breast cancer cells. Previous reports have correlated transcriptional activity with increased acetylation of Sp1 (Torigoe *et al.*, 2005). However, studies by Waby *et al.* (2010) suggested that exposure to butyrate (a known HDACI) elevated p21 expression by increasing acetylation of Sp1, which prevented Sp1 binding to the p21 promoter. ChIP analysis indicated that Sp1 acetylation induced by trichostatin A, another HDACI, inhibited its DNA binding at promoters of 12(S)-lipoxygenase, leading to a diminished level of this enzyme (Chen *et al.*, 2008). To date, there still remains a controversy on the relationship between acetylated Sp1 and its transcriptional potency. Our results would support the proposition 'the more acetylation, the less transcriptional activation', as LW479 exposure increased both the dissociation of Sp1 from the EGFR promoter and the acetylation of Sp1. The constitutively low-acetylated Sp1 we observed in MDA-231 cells might therefore play a role in the transcription of EGFR in breast cancer.

Our *in vivo* studies showed that LW479 was effective in breast cancer xenograft models. We observed a diminished expression of EGFR and an increased level of acetylated histone H3 in primary tumour tissues following treatment with LW479 (40 $mg \cdot kg^{-1}$), indicating that the actions of LW479 in xenograft models was target specific. Although LW479 was effective in suppresiing breast tumour growth, the results are not particularly impressive as the inhibition rate was only about 40%. One possible reason may lie in the daily dose of LW479. An earlier study showed that SAHA as well as other novel hydroxamate-based HDACIs exhibited potent anti-breast tumour activity at a daily dose of 90 $mg \cdot kg^{-1}$ (Zhang *et al.*, 2011) while the maximum dose of LW479 we used was 40 $mg \cdot kg^{-1}$. However, this dose of LW479 showed significant inhibition of tumour metastasis in both spontaneous and experimental metastasis models (Figures 4 and 5). Therefore, LW479 may be a potential anti-metastatic agent. The epithelial-mesenchymal transition (EMT), a process by which epithelial cells lose their epithelial charac-

teristics and acquire mesenchymal-like phenotypes, endows cells with invasive properties. Accumulating evidence has indicated that the EMT is a relevant and important process in tumour metastasis (Ombrato and Malanchi, 2014). We found that LW479 up-regulated epithelial markers and down-regulated mesenchymal markers in highly mesenchymal-like MDA-231 cells, suggesting that LW479 could reverse the EMT and act as a metastasis inhibitor (Supporting Information Fig. S8). In addition, preclinical studies using cell-based assay have revealed that EGFR inhibitors in combination with cytotoxic chemotherapies resulted in little effect (Corkery *et al.*, 2009) and a phase II clinical trial in TNBC patients indicated that compounds targeting EGFR showed no obvious benefit in survival (Carey *et al.*, 2012). Lee *et al.* (2012) emphasized that sequential, rather than concurrent, application of EGFR inhibitors and DNA-damaging agents sensitized breast cancer cells to death. Besides, in clinical settings, HDACIs have shown only moderate effects as single-agent anticancer therapies (Bots and Johnstone, 2009). Considering all these aspects, the therapeutic potential of LW479 may be best fulfilled through appropriate combinations with other chemotherapeutic agents.

In conclusion, our studies suggested that LW479 possesses the potential for inhibiting breast cancer progression and that it acts by diminishing levels of EGFR. However, it appears that EGFR is not the only target gene of LW479 in breast cancer cells. Further investigations are needed to identify other genes and proteins interacting with LW479, which will give us a better understanding of the molecular basis of breast cancer inhibition by LW479.

Acknowledgements

This study was partially supported by Major State Basic Research Development Program of China (2015CB910400, 2012CB910401), National Natural Science Foundation of China (81472788, 81272463, 81202407, 81330049), National Major Scientific and Technological Special Project for 'Significant New Drugs Development' (2013ZX09507001) and Innovation Program of Shanghai Municipal Education Commission (13zz034).

Author contributions

J. L., T. Z. and F. Y. performed the research. Y. C., M. L., Z. Y. and J. L. designed the research study. F. D., F. Y. and Y. C. contributed essential reagents or tools. J. L., T. Z., Y. H., D. G., Y. C. and Z. Y. analysed the data. J. L., Y. C., M. L. and Z. Y. wrote the paper.

Conflict of interest

The authors declare no conflicts of interest.

References

Alexander SPH, Benson HE, Faccenda E, Pawson AJ, Sharman JL, Spedding M *et al.* (2013a). The Concise Guide to PHARMACOLOGY 2013/14: Enzymes. Br J Pharmacol 170: : 1797–1867.

Alexander SPH, Benson HE, Faccenda E, Pawson AJ, Sharman JL, Spedding M *et al.* (2013b). The Concise Guide to PHARMACOLOGY 2013/14: Catalytic Receptors. Br J Pharmacol 170: , 1676–1705.

Altenburg BC, Via DP, Steiner SH (1976). Modification of the phenotype of murine sarcoma virus-transformed cells by sodium butyrate. Effects on morphology and cytoskeletal elements. Exp Cell Res 102: 223–231.

Arnesen T (2011). Towards a functional understanding of protein N-terminal acetylation. PLoS Biol 9: e1001074.

Avraham R, Yarden Y (2011). Feedback regulation of EGFR signalling: decision making by early and delayed loops. Nat Rev Mol Cell Biol 12: 104–117.

Baselga J (2002). Combined anti-EGF receptor and anti-HER2 receptor therapy in breast cancer: a promising strategy ready for clinical testing. Ann Oncol 13: 8–9.

Bolden JE, Peart MJ, Johnstone RW (2006). Anticancer activities of histone deacetylase inhibitors. Nat Rev Drug Discov 5: 769–784.

Bots M, Johnstone RW (2009). Rational combinations using HDAC inhibitors. Clin Cancer Res 15: 3970–3977.

Brandt B, Meyer-Staeckling S, Schmidt H, Agelopoulos K, Buerger H (2006). Mechanisms of egfr gene transcription modulation: relationship to cancer risk and therapy response. Clin Cancer Res 12: 7252–7260.

Byler S, Goldgar S, Heerboth S, Leary M, Housman G, Moulton K *et al.* (2014). Genetic and epigenetic aspects of breast cancer progression and therapy. Anticancer Res 34: 1071–1077.

Carey LA, Rugo HS, Marcom PK, Mayer EL, Esteva FJ, Ma CX *et al.* (2012). TBCRC 001: randomized phase II study of cetuximab in combination with carboplatin in stage IV triple-negative breast cancer. J Clin Oncol 30: 2615–2623.

Chen CJ, Chang WC, Chen BK (2008). Attenuation of c-Jun and Sp1 expression and p300 recruitment to gene promoter confers the trichostatin A-induced inhibition of 12(S)-lipoxygenase expression in EGF-treated A431 cells. Eur J Pharmacol 591: 36–42.

Chou CW, Wu MS, Huang WC, Chen CC (2011). HDAC inhibition decreases the expression of EGFR in colorectal cancer cells. PLoS ONE 6: e18087.

Corkery B, Crown J, Clynes M, O'Donovan N (2009). Epidermal growth factor receptor as a potential therapeutic target in triple-negative breast cancer. Ann Oncol 20: 862–867.

Dai F, Chen Y, Song Y, Huang L, Zhai D, Dong Y *et al.* (2012). A natural small molecule harmine inhibits angiogenesis and suppresses tumour growth through activation of p53 in endothelial cells. PLoS ONE 7: e52162.

Deroanne CF, Bonjean K, Servotte S, Devy L, Colige A, Clausse N *et al.* (2002). Histone deacetylases inhibitors as anti-angiogenic agents altering vascular endothelial growth factor signaling. Oncogene 21: 427–436.

Dong Y, Lu B, Zhang X, Zhang J, Lai L, Li D *et al.* (2010). Cucurbitacin E, a tetracyclic triterpenes compound from Chinese medicine, inhibits tumor angiogenesis through VEGFR2-mediated Jak2-STAT3 signaling pathway. Carcinogenesis 31: 2097–2104.

Esteller M (2007). Cancer epigenomics: DNA methylomes and histone- modification maps. Nat Rev Genet 8: 286–298.

Gediya LK, Chopra P, Purushottamachar P, Maheshwari N, Njar VC (2005). A new simple and high-yield synthesis of suberoylanilide hydroxamic acid and its inhibitory effect alone or in combination with retinoids on proliferation of human prostate cancer cells. J Med Chem 48: 5047–5051.

Ginsburg E, Salomon D, Sreevalsan T, Freese E (1973). Growth inhibition and morphological changes caused by lipophilic acids in mammalian cells. Proc Natl Acad Sci U S A 70: 2457–2461.

Glaser KB, Li J, Aakre ME, Morgan DW, Sheppard G, Stewart KD *et al.* (2002). Transforming growth factor beta mimetics: discovery of 7-[4-(4-cyanophenyl) phenoxy]-heptanohydroxamic acid, a biaryl hydroxamate inhibitor of histone deacetylase. Mol Cancer Ther 1: 759–768.

Huang Y, Nayak S, Jankowitz R, Davidson NE, Oesterreich S (2011). Epigenetics in breast cancer: what's new? Breast Cancer Res 13: 225.

Jang ER, Lim SJ, Lee ES, Jeong G, Kim TY, Bang Y *et al.* (2004). The histone deacetylase inhibitor trichostatin A sensitizes estrogen receptor alpha-negative breast cancer cells to tamoxifen. Oncogene 23: 1724–1736.

Khan O, La Thangue NB (2012). HDAC inhibitors in cancer biology: emerging mechanisms and clinical applications. Immunol Cell Biol 90: 85–94.

Kilkenny C, Browne W, Cuthill IC, Emerson M, Altman DG (2010). Animal research: reporting in vivo experiments: the ARRIVE guidelines. Br J Pharmacol 160: 577–1579.

Lee GY, Kenny PA, Lee EH, Bissell MJ (2007). Three-dimensional culture models of normal and malignant breast epithelial cells. Nat Methods 4: 359–365.

Lee MJ, Ye AS, Gardino AK, Heijink AM, Sorger PK, MacBeath G *et al.* (2012). Sequential application of anticancer drugs enhances cell death by rewiring apoptotic signaling networks. Cell 149: 780–794.

Liu W, Innocenti F, Wu MH, Desai AA, Dolan ME, Cook EH *et al.* (2005). A functional common polymorphism in a Sp1 recognition site of the epidermal growth factor receptor gene promoter. Cancer Res 65: 46–53.

Lu J, Guo H, Treekitkarnmongkol W, Li P, Zhang J, Shi B *et al.* (2009). 14-3-3zeta cooperates with ErbB2 to promote ductal carcinoma in situ progression to invasive breast cancer by inducing epithelial-mesenchymal transition. Cancer Cell 16: 195–207.

Lu Z, Jiang G, Blume-Jensen P, Hunter T (2001). Epidermal growth factor-induced tumor cell invasion and metastasis initiated by dephosphorylation and downregulation of focal adhesion kinase. Mol Cell Biol 21: 4016–4031.

Marks P, Rifkind RA, Richon VM, Breslow R, Miller T, Kelly WK (2001). Histone deacetylases and cancer: causes and therapies. Nat Rev Cancer 1: 194–202.

Masuda H, Zhang D, Bartholomeusz C, Doihara H, Hortobagyi GN, Ueno NT (2012). Role of epidermal growth factor receptor in breast cancer. Breast Cancer Res Treat 136: 331–345.

McGrath JC, Drummond GB, McLachlan EM, Kilkenny C, Wainwright CL (2010). Guidelines for reporting experiments involving animals: the ARRIVE guidelines. Br J Pharmacol 160: 1573–1576.

Minucci S, Pelicci PG (2006). Histone deacetylase inhibitors and the promise of epigenetic (and more) treatments for cancer. Nat Rev Cancer 6: 38–51.

Mottet D, Bellahcene A, Pirotte S, Waltregny D, Deroanne C, Lamour V *et al.* (2007). Histone deacetylase 7 silencing alters endothelial cell migration, a key step in angiogenesis. Circ Res 101: 1237–1246.

Munster PN, Thurn KT, Thomas S, Raha P, Lacevic M, Miller A *et al.* (2011). A phase II study of the histone deacetylase inhibitor vorinostat combined with tamoxifen for the treatment of patients with hormone therapy-resistant breast cancer. Br J Cancer 104: 1828–1835.

Nishi H, Nishi KH, Johnson AC (2002). Early Growth Response-1 gene mediates up-regulation of epidermal growth factor receptor expression during hypoxia. Cancer Res 62: 827–834.

Ombrato L, Malanchi I (2014). The EMT universe: space between cancer cell dissemination and metastasis initiation. Crit Rev Oncog 19: 349–361.

Pawson AJ, Sharman JL, Benson HE, Faccenda E, Alexander SP, Buneman OP *et al.*; NC-IUPHAR (2014). The IUPHAR/BPS Guide to PHARMACOLOGY: an expert-driven knowledge base of drug targets and their ligands. Nucl. Acids Res 42 (Database Issue): D1098–D1106.

Pitteri SJ, Amon LM, Busald Buson T, Zhang Y, Johnson MM, Chin A *et al.* (2010). Detection of elevated plasma levels of epidermal growth factor receptor before breast cancer diagnosis among hormone therapy users. Cancer Res 70: 8598–8606.

Pulukuri SM, Gorantla B, Rao JS (2007). Inhibition of histone deacetylase activity promotes invasion of human cancer cells through activation of urokinase plasminogen activator. J Biol Chem 282: 35594–35603.

Rossig L, Li H, Fisslthaler B, Urbich C, Fleming I, Forstermann U *et al.* (2002). Inhibitors of histone deacetylation downregulate the expression of endothelial nitric oxide synthase and compromise endothelial cell function in vasorelaxation and angiogenesis. Circ Res 91: 837–844.

Sasakawa Y, Naoe Y, Noto T, Inoue T, Sasakawa T, Matsuo M *et al.* (2003). Antitumor efficacy of FK228, a novel histone deacetylase inhibitor, depends on the effect on expression of angiogenesis factors. Biochem Pharmacol 66: 897–906.

Schrump DS (2009). Cytotoxicity mediated by histone deacetylase inhibitors in cancer cells: mechanisms and potential clinical implications. Clin Cancer Res 15: 3947–3957.

Su GH, Sohn TA, Ryu B, Kern SE (2000). A novel histone deacetylase inhibitor identified by high-throughput transcriptional screening of a compound library. Cancer Res 60: 3137–3142.

Tan NY, Khachigian LM (2009). Sp1 phosphorylation and its regulation of gene transcription. Mol Cell Biol 29: 2483–2488.

Tate CR, Rhodes LV, Segar HC, Driver JL, Pounder FN, Burow ME *et al.* (2012). Targeting triple-negative breast cancer cells with the histone deacetylase inhibitor panobinostat. Breast Cancer Res 14: R79.

Torigoe T, Izumi H, Wakasugi T, Niina I, Igarashi T, Yoshida T *et al.* (2005). DNA topoisomerase II poison TAS-103 transactivates GC-box-dependent transcription via acetylation of Sp1. J Biol Chem 280: 1179–1185.

Turner CE (2000). Paxillin and focal adhesion signalling. Nat Cell Biol 2: E231–E236.

Varshochi R, Halim F, Sunters A, Alao JP, Madureira PA, Hart SM *et al.* (2005). ICI182,780 induces p21Waf1 gene transcription through releasing histone deacetylase 1 and estrogen receptor alpha from Sp1 sites to induce cell cycle arrest in MCF-7 breast cancer cell line. J Biol Chem 280: 3185–3196.

Waby JS, Chirakkal H, Yu C, Griffiths GJ, Benson RS, Bingle CD *et al.* (2010). Sp1 acetylation is associated with loss of DNA binding at promoters associated with cell cycle arrest and cell death in a colon cell line. Mol Cancer 9: 275.

Wheeler DL, Dunn EF, Harari PM (2010). Understanding resistance to EGFR inhibitors-impact on future treatment strategies. Nat Rev Clin Oncol 7: 493–507.

Xu WS, Parmigiani RB, Marks PA (2007). Histone deacetylase inhibitors: molecular mechanisms of action. Oncogene 26: 5541–5552.

Zhang T, Li J, Dong Y, Zhai D, Lai L, Dai F *et al*. (2012). Cucurbitacin E inhibits breast tumor metastasis by suppressing cell migration and invasion. Breast Cancer Res Treat 135: 445–458.

Zhang T, Chen Y, Li J, Yang F, Wu H, Dai F *et al*. (2014). Antitumor action of a novel histone deacetylase inhibitor, YF479, in breast cancer. Neoplasia 16: 665–677.

Zhang Y, Fang H, Feng J, Jia Y, Wang X, Xu W (2011). Discovery of a tetrahydroisoquinoline-based hydroxamic acid derivative (ZYJ-34c) as histone deacetylase inhibitor with potent oral antitumor activities. J Med Chem 54: 5532–5539.

Zhou Q, Shaw PG, Davidson NE (2009). Inhibition of histone deacetylase suppresses EGF signaling pathways by destabilizing EGFR mRNA in ER-negative human breast cancer cells. Breast Cancer Res Treat 117: 443–451.

Supporting information

Additional Supporting Information may be found in the online version of this article at the publisher's web-site:

http://dx.doi.org/10.1111/bph.13165

Figure S1 The synthesis of LW479. Regents and conditions: (A) 3-bromobenzaldehyde, EtOH, 0°C then to room temperature; (B) $NaBH_4$, 0°C then to room temperature; (C) pimelic acid anhydride, 1,4-dioxane, reflux; (D) MeOH, Cat.$SOCl_2$, reflux; (E) $NH_2OH.HCl$, MeOH, KOH. The intermediate 2-(3-bromophenyl)-3-(2-hydroxyphenyl)-4-thiazolidinone (2) was constructed from o-aminophenol (1), 3-bromobenzaldehyde and thioglycolic acid, which was alkylated with 6-bromine caproic acid methyl ester to yield ester compound (3), and the ester groups were treated with NH_2OH•HCl in methanol to get the compound LW479. All starting reagents and materials were purchased from commercial sources and used without further purification. All reactions were monitored by TLC and UV spectra, column chromatography was performed on silica gel, NMR spectra was recorded on a Bruker 300 or 500 MHz instrument and obtained as $CDCl_3$ DMSO-d6 solutions (reported in p.p.m.), using DMSO-d6 as the reference standard (2.50 p.p.m.). Mass spectral data (ESI) were gathered on VG ZAB-HS or VG-7070 instrument. HPLC (Agilent Technologies 1200 Series) was utilized for purification, injection volume was 10 L, flow rate of 1.5 mL/min, solvent A: H_2O; solvent B: MeOH; gradient of 40–90% B (0–10 min), 90% B (10–15 min), 90–40% B (15–20 min). Compound purity was determined by HPLC with a confirming purity of ≥98% for the testing compounds.

Figure S2 ^{1}HMR spectrum of LW479. ^{1}H NMR (DMSO, 300 MHz): δ 10.39 (brs, 1H), 8.69 (brs, 1H), 7.63 (s, 1H), 7.41 (dd, J = 9.0, 9.0 Hz, 2H), 7.24 (d, J = 7.8 Hz, 1H), 7.19 (d, J = 7.8 Hz, 1H), 7.02 (d, J = 7.8 Hz, 2H), 6.82 (dd, J = 7.5, 7.5 Hz, 1H), 6.16 (s, 1H), 4.03 (d, J = 15.6 Hz, 1H), 3.96-3.91(m, 2H), 3.81 (d, J = 15.6 Hz, 1H), 2.03-1.98 (m, 2H), 1.79-1.75 (m, 2H), 1.64-1.57 (m, 2H), 1.50-1.42 (m, 2H).

Figure S3 ^{13}C NMR spectrum of LW479. ^{13}C NMR (DMSO, 125 MHz) δ 170.41, 169.04, 154.17, 142.67, 131.47, 130.59, 130.02, 129.33, 126.52, 125.58, 121.56, 120.24, 113.15, 67.79, 62.60, 32.29, 32.06, 28.42, 25.16, 24.91.

Figure S4 LW479 induces histone acetylation and breast cancer cell apoptosis. (A) LW479 up-regulated histone H3 acetylation in a dose-dependent manner. (B, C) LW479 (10μM)-induced cell apoptosis and the expression of cleaved caspase 3.

Figure S5 Cytotoxicity of SAHA. MDA-231 cells were seeded in 96-well plate and treated with different concentrations of SAHA for 48 h. Aqueous One Solution (20 μL) was subsequently added and the absorption at 490 nm was measured by a microplate spectrophotometer.

Figure S6 LW479 inhibits EGFR expression via regulating Sp1-dependent EGFR transcription. (A, B) MDA-231 cells were transfected with Sp1 siRNAs. Forty-eight hours post-transfection, cells were harvested. RT-PCR or Western blot analysis was used for detecting Sp1 and EGFR expression. (C, D) MDA-231 cells were transfected with p3xFLAG-Sp1 vector. After 48 h, cells were left treated or untreated with LW479 (10 μM) for another 24 h. RT-PCR or Western blot analysis was used for detecting Sp1 and EGFR expression. (E) MDA-231 cells were transfected with EGFR-Luc and treated with different concentrations of LW479 for 24 h. The results were normalized to the *Renilla* luciferase activity. (F) LW479 dose-dependently inhibited DNA-binding activity of Sp1 in MDA-231 cells. Nuclear extract was prepared and examined by EMSA assay. '1#' represents negative control; '2#' represents 100-fold cold probe competition. Three independent experiments were carried out.

Figure S7 LW479 has little effect on body weight of mice.

Figure S8 LW479 affects EMT-related protein expression. MDA-231 cells were treated with different concentrations of LW479 for 48 h; cells were then harvested with RIPA. Western blot analysis was performed with specific antibodies.

Figure S9 A proposed diagram of EGFR down-regulation by LW479. In human breast cancer cells, low-acetylated Sp1 recruits HDAC1 to the EGFR promoter and transcription activation. Inhibition of HDAC activity by LW479 increases the acetylation level of Sp1 and disrupts the interaction of Sp1 with HDAC1, leading to transcription repression of EGFR.